



PAPER

Quantum collisional thermostats

OPEN ACCESS

RECEIVED
22 September 2021REVISED
16 December 2021ACCEPTED FOR PUBLICATION
7 January 2022PUBLISHED
15 February 2022

Original content from
this work may be used
under the terms of the
[Creative Commons
Attribution 4.0 licence](#).

Any further distribution
of this work must
maintain attribution to
the author(s) and the
title of the work, journal
citation and DOI.



Jorge Tabanera^{1,*} , Inés Luque¹, Samuel L Jacob^{2,3}, Massimiliano Esposito^{2,3},
Felipe Barra^{3,4} and Juan M R Parrondo¹

¹ Departamento de Estructura de la Materia, Física Térmica y Electrónica and GISC, Universidad Complutense de Madrid, 28040 Madrid, Spain

² Complex Systems and Statistical Mechanics, Physics and Materials Science Research Unit, University of Luxembourg, L-1511 Luxembourg, G.D., Luxembourg

³ Kavli Institute for Theoretical Physics, University of California, Santa Barbara, CA 93106 Santa Barbara, United States of America

⁴ Departamento de Física, Facultad de Ciencias Físicas y Matemáticas, Universidad de Chile, 837.0415 Santiago, Chile

* Author to whom any correspondence should be addressed.

E-mail: jorgetab@ucm.es, samuel.lourenco@uni.lu, massimiliano.esposito@uni.lu, fbarra@dfi.uchile.cl
and parrondo@fis.ucm.es

Keywords: quantum thermodynamics, quantum thermostats, collisional reservoirs, open quantum systems

Abstract

Collisional reservoirs are becoming a major tool for modelling open quantum systems. In their simplest implementation, an external agent switches on, for a given time, the interaction between the system and a specimen from the reservoir. Generically, in this operation the external agent performs work onto the system, preventing thermalization when the reservoir is at equilibrium. One can recover thermalization by considering an autonomous global setup where the reservoir particles colliding with the system possess a kinetic degree of freedom. The drawback is that the corresponding scattering problem is rather involved. Here, we present a formal solution of the problem in one dimension and for flat interaction potentials. The solution is based on the transfer matrix formalism and allows one to explore the symmetries of the resulting scattering map. One of these symmetries is micro-reversibility, which is a condition for thermalization. We then introduce two approximations of the scattering map that preserve these symmetries and, consequently, thermalize the system. These relatively simple approximate solutions constitute models of quantum thermostats and are useful tools to study quantum systems in contact with thermal baths. We illustrate their accuracy in a specific example, showing that both are good approximations of the exact scattering problem even in situations far from equilibrium. Moreover, one of the models consists of the removal of certain coherences plus a very specific randomization of the interaction time. These two features allow one to identify as heat the energy transfer due to switching on and off the interaction. Our results prompt the fundamental question of how to distinguish between heat and work from the statistical properties of the exchange of energy between a system and its surroundings.

1. Introduction

A proper understanding of the interaction between a system and a thermal reservoir is crucial for the development of thermodynamics. This interaction turns out to be more involved for quantum systems. The theory of quantum open systems was initiated more than fifty years ago and has provided robust and widely used tools, such as the Lindblad equation for autonomous systems weakly coupled to thermal baths [1–3]. However, there are a number of questions which are still open or even under some controversy. Examples are Lindblad equations for driven systems [4], local versus global Lindblad and master equations [5, 6], strong coupling [7, 8], and non-Markovian effects [9].

Some of these issues could be addressed and eventually clarified if we had simplified and analytically solvable models of the interaction between a quantum system and a thermal bath. Good candidates are the so-called repeated-interaction or collisional reservoirs [10–13]. In these models, the system does not

interact with the reservoir as a whole. The reservoir consists of a large ensemble of independent units in a given state (usually, the equilibrium Gibbs state). One unit is extracted and put in contact with the system during a certain time interval. The process is repeated with fresh units, i.e. in each interaction the initial state of the unit is always the same and given by the density matrix that characterizes the reservoir. The interaction induces a quantum map in the system, which is exact and usually simpler to analyze than a continuous-time Lindblad equation. Moreover, this type of interaction occurs in relevant experimental setups, as in cavity quantum electrodynamics [14].

However, this approach has a drawback. The models explored up to now are not autonomous: an external agent is needed to switch on and off the interaction between the system and the unit. In general, this action involves an energy exchange, which is a work supply that prevents the system from thermalizing [10–13] (here, thermalization is understood as the relaxation towards the equilibrium Gibbs state; we do not consider more involved situations where a strong coupling between the system and the environment can drive the former to non-standard equilibrium states [15]).

More recently, Cattaneo *et al* [16] have proved that any Lindbladian dynamics can be reproduced by a specifically engineered repeated-interaction scheme. In particular, Lindblad equations arising from standard weak coupling approximations and inducing thermalization can be implemented using the prescription derived in [16]. This is a remarkable and interesting method to obtain repeated-interaction thermostats, although the resulting energetics is not yet clear. Notice also that, in this approach, a well-established Lindblad equation inducing thermalization is necessary as a starting point. Another related work is reference [17], where a repeated interaction scheme based on periodically refreshed baths is introduced and proved to converge to the exact dynamics of an arbitrary open quantum system, even in situations far from equilibrium and/or from the Markovian or weak coupling regimes. In particular, if the system is in contact with an equilibrium reservoir, this scheme induces thermalization. In this approach, the units are in fact full finite baths, whose global state is refreshed in each interaction. If the duration of the interaction is much larger than the memory time of the bath, then the work performed by switching on and off the coupling is negligible and one recovers thermalization.

In a series of papers [18, 19], we adopted a different strategy and managed to build a repeated interaction scheme with zero work by considering a fully autonomous scenario, where the units escape from the reservoir with a random velocity given by the effusion distribution, move in space as quantum wave packets, and collide with the system without the need of an external agent. In this case, the energy to switch on and off the interaction is provided by the spatial degree of freedom of the unit. It turns out that the width of the incident wave packets in momentum representation plays a crucial role in the thermodynamics of the whole setup [18]. For wave packets with a large momentum dispersion, the exchanged energy can be interpreted as work [20]. On the other hand, if one assumes that the velocity of the unit is in equilibrium and that the wave packets are narrow enough in momentum representation, then this energy exchange is no longer work but heat, and the system thermalizes [18]. Consequently, this latter approach captures all the essential features of a real thermostat.

In this paper, we extend the analysis of our previous work [18] to include the internal degrees of freedom of the units. Then we apply the transfer matrix formalism [21] to obtain an exact solution of the scattering problem for a uniform interaction potential. This solution allows us to explore the symmetries of the scattering map. In particular, we analyze the role of micro-reversibility as a sufficient condition for the system to thermalize when it is bombarded by narrow wave packets with velocities distributed according to the effusion distribution [18, 19].

We then find approximations to the exact scattering map for high incident kinetic energy. The approximations preserve micro-reversibility and, consequently, induce thermalization when the particles come from a reservoir at equilibrium. The first approximation is based on wave-vector operators (WVOs) and can be further simplified for large kinetic energy. The final result is a scattering map that resembles the repeated-interaction scheme, where the interaction Hamiltonian acts during a given time. When the system is bombarded by effusion particles, this time is a random variable whose distribution depends on the total energy of the system and the unit. This very specific randomization of the interaction time, plus the decoupling of populations and coherences by narrow wave packets [18], allows one to interpret the energy exchanged in the switching of the interaction as heat. Recall that, in the standard non-autonomous repeated interaction schemes [11], the energy transfer between the system and the external agent that switches on and off the interaction is work. In contrast, in our models this energy is heat because it is exchanged with the kinetic degree of freedom of the unit, which is in thermal equilibrium. Our results show that the distinction between heat and work is reflected in the dynamics of the system. This raises the interesting question of whether the energy exchange between a generic open system (classical or quantum) and its surroundings can be characterized as work or heat just by analyzing the dynamics of this exchange.

The paper is organized as follows. Section 2 is essentially a review of the results of our previous paper [18]: we discuss the map induced on the system by a single collision with a unit consisting of a wave packet, as well as the sufficient conditions for this map to thermalize the system when the incident velocity is random. The relation between these conditions and the symmetries of the scattering matrix is discussed in this section and in appendix B. Section 3 is devoted to the transfer matrix method, a technique to solve scattering problems in one dimension. The transfer matrix method allows us to obtain a formal expression of the scattering matrix and to derive, in subsection 3.3, an approximation for high incident energy, which is the basis of the thermostats presented in the next section, section 4. There we also show that this approximation and the resulting thermostats fulfill the symmetry conditions for thermalization. Finally, we apply the results to a specific example in section 5 and present our main conclusions in section 6.

2. Thermalization and the scattering map

2.1. Collisional reservoirs

We consider units drawn from a reservoir and colliding, one by one, with the system [18]. Each unit U is a particle of mass m with internal states and moving in one dimension. Its corresponding Hilbert space is $\mathcal{H}_U = \mathcal{H}_{U,p} \otimes \mathcal{H}_{U,int}$, where $\mathcal{H}_{U,p}$ refers to the spatial states and $\mathcal{H}_{U,int}$ is the space of internal states. The units collide with the system S , which only has internal degrees of freedom and whose states are vectors in the Hilbert space \mathcal{H}_S .

The system is a fixed scatterer located in an interval $[-L/2, L/2]$, as sketched in figure 1. The whole setup is described by the following Hamiltonian H_{tot} , which is an operator acting on $\mathcal{H}_U \otimes \mathcal{H}_S$:

$$H_{tot} = \frac{\hat{p}^2}{2m} + \chi_L(\hat{x})H_{US} + H_U + H_S. \quad (1)$$

\hat{p} and \hat{x} being, respectively, the momentum and position operators in $\mathcal{H}_{U,p}$. $\chi_L(x)$ is the indicator function of the scattering region $[-L/2, L/2]$: $\chi_L(x) = 1$ if $x \in [-L/2, L/2]$ and zero otherwise. Outside the scattering region, the free Hamiltonian $H_0 = H_U + H_S$ rules the evolution of the internal degrees of freedom and is the sum of the Hamiltonian of the system H_S and of the internal degrees of freedom of the unit H_U . Within the scattering region, the Hamiltonian affecting the internal degrees of freedom is $H = H_{US} + H_0$, which we will call total internal Hamiltonian. The free and the total internal Hamiltonians, H_0 and H respectively, are operators in $\mathcal{H}_{U,int} \otimes \mathcal{H}_S$. We will assume that both have a discrete spectrum with eigenstates:

$$\begin{aligned} H_0|s_J\rangle &= e_J|s_J\rangle \\ H|s'_J\rangle &= e'_J|s'_J\rangle. \end{aligned} \quad (2)$$

Notice that $\{|s_J\rangle\}$ and $\{|s'_J\rangle\}$ are orthonormal basis of the Hilbert space of the internal states of the unit and the system, $\mathcal{H}_{U,int} \otimes \mathcal{H}_S$. Moreover, the eigenvectors of H_0 can be written as $|s_J\rangle = |s_{j_U}\rangle_U \otimes |s_{j_S}\rangle_S \in \mathcal{H}_{U,int} \otimes \mathcal{H}_S$, with

$$\begin{aligned} H_U|s_{j_U}\rangle_U &= e_{j_U}^{(U)}|s_{j_U}\rangle_U \\ H_S|s_{j_S}\rangle_S &= e_{j_S}^{(S)}|s_{j_S}\rangle_S \end{aligned} \quad (3)$$

and total energy $e_J = e_{j_U}^{(U)} + e_{j_S}^{(S)}$. Here and in the rest of the paper, we use capital letters J for the quantum numbers labelling the eigenstates of H_0 and H , and lower case letters, j_U, j_S , for the quantum numbers corresponding to H_U and H_S . In this notation, the quantum number J of an eigenstate of H_0 comprises the two quantum numbers $J = (j_S, j_U)$.

In order to observe well-defined collisions, the spatial state of the units must be a wave packet $|\phi_{p_0, x_0}\rangle$ centered around position x_0 and momentum p_0 , with momentum dispersion σ_p , as the one depicted in figure 1. An example is the Gaussian wave packet, whose wave function in momentum representation reads [18]

$$\langle p|\phi_{p_0, x_0}\rangle = (2\pi\sigma_p^2)^{-1/4} \exp\left[-\frac{(p-p_0)^2}{4\sigma_p^2} - i\frac{px_0}{\hbar}\right]. \quad (4)$$

Here $|p\rangle$ denotes the non-normalizable plane wave with momentum p . The Hamiltonian (1) is invariant under spatial reflection, $(\hat{x}, \hat{p}) \rightarrow (-\hat{x}, -\hat{p})$, since the indicator function of the interval $[-L/2, L/2]$ is even: $\chi_L(x) = \chi_L(-x)$. Consequently, a collision with a unit coming from the left with positive velocity, $x_0 < 0$ and $p_0 > 0$, is equivalent to the mirror collision with a unit $|\phi_{-p_0, -x_0}\rangle$ coming from the right. Hence, we can limit our discussion to units with positive velocity, without loss of generality (the mathematical consequences of this spatial symmetry in the scattering problem are explained in detail in appendix B2).

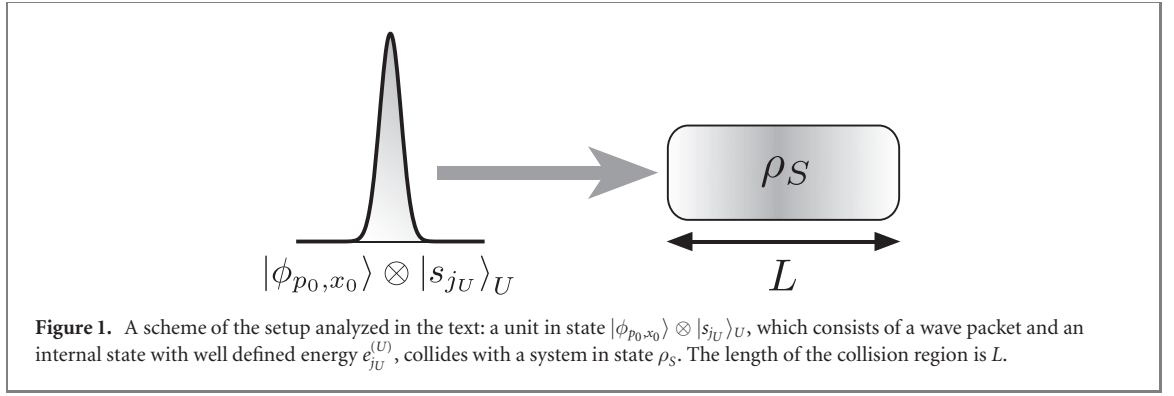


Figure 1. A scheme of the setup analyzed in the text: a unit in state $|\phi_{p_0, x_0}\rangle \otimes |s_{j_U}\rangle_U$, which consists of a wave packet and an internal state with well defined energy $e_{j_U}^{(U)}$, collides with a system in state ρ_S . The length of the collision region is L .

The internal state of the unit is disentangled from the system and depends on the properties of the reservoir. For instance, if the reservoir is in thermal equilibrium at inverse temperature β , the internal state is the Gibbs state $\rho_{U,eq} = e^{-\beta H_U} / Z_U$, where Z_U is the corresponding partition function. We first analyze the case of a unit in a pure eigenstate of H_U , $|s_{j_U}\rangle_U$, and later on we consider thermal mixtures of these eigenstates.

2.2. The scattering map

The effect of the collision on the system is given by a CPTP map, which depends on the incident momentum p_0 and the internal state of the unit. However, it is convenient to consider first the effect of the collision on all the internal degrees of freedom, those of the system and of the internal state of the unit, following reference [18]. The scattering map \mathbb{S} relates the internal state before the collision, ρ , and after, $\rho' = \mathbb{S}\rho$. Expressing the states in the eigenbasis of H_0 , $\rho_{JK} = \langle s_J | \rho | s_K \rangle$ and $\rho'_{JK} = \langle s_J | \rho' | s_K \rangle$, the scattering map is given by a tensor $\mathbb{S}_{J'K'}^{JK}$ such that

$$\rho'_{J'K'} = \sum_{J,K} \mathbb{S}_{J'K'}^{JK} \rho_{JK}. \quad (5)$$

In reference [18], we have analyzed in detail this scattering map and found that the behavior of the state ρ crucially depends on the momentum dispersion of the packet, σ_p . If the dispersion is small enough, the outgoing wave packets corresponding to different transitions $|s_J\rangle \rightarrow |s_{J'}\rangle$ are either identical or do not overlap. The precise condition for these narrow wave packets, in terms of the transition energies $\Delta_{JJ'} = e_J - e_{J'}$, reads

$$\sigma_p \ll \frac{m|\Delta_{JJ'} - \Delta_{KK'}|}{2p_0} \quad (6)$$

for every pair of transitions $|s_J\rangle \rightarrow |s_{J'}\rangle$ and $|s_K\rangle \rightarrow |s_{K'}\rangle$ with $\Delta_{JJ'} \neq \Delta_{KK'}$. If the incident packet fulfills this condition, we call it narrow wave packet and the scattering map induced by the collision is given by [18]:

$$\begin{aligned} \mathbb{S}_{J'K'}^{JK} &\simeq t_{JJ'}(E_{p_0} + e_J) [t_{K'K}(E_{p_0} + e_K)]^* \\ &+ r_{JJ'}(E_{p_0} + e_J) [r_{K'K}(E_{p_0} + e_K)]^*, \end{aligned} \quad (7)$$

whenever

$$e_{J'} - e_J = e_{K'} - e_K \quad (8)$$

and $E_{p_0} + e_J \geq e_{J'}$, and zero otherwise. Here $t_{JJ'}(E)$ and $r_{JJ'}(E)$ are the transmission and reflection amplitudes that depend on the total energy, kinetic $E_{p_0} \equiv p_0^2/(2m)$ plus internal e_J . They are defined for all J and J' such that $e_J, e_{J'} \leq E$, which are the so-called open channels in the collision and span the Hilbert subspace

$$\mathcal{H}_{\text{open}} = \text{lin}\{|s_J\rangle : e_J \leq E\} \subseteq \mathcal{H}_{U,\text{int}} \otimes \mathcal{H}_S. \quad (9)$$

For Hamiltonians that are invariant under spatial reflection, $(\hat{x}, \hat{p}) \rightarrow (-\hat{x}, -\hat{p})$, the transmission and reflection amplitudes are usually arranged into two matrices $\mathbf{t}(E)$ and $\mathbf{r}(E)$ that form the scattering matrix (see appendix B2):

$$\tilde{\mathcal{S}}(E) = \begin{pmatrix} \mathbf{r}(E) & \mathbf{t}(E) \\ \mathbf{t}(E) & \mathbf{r}(E) \end{pmatrix}. \quad (10)$$

The two matrices $\mathbf{t}(E)$ and $\mathbf{r}(E)$ are defined on the subspace of open channels $\mathcal{H}_{\text{open}}$. One important property of the scattering matrix is that it is unitary on the subspace $\mathcal{H}_{\text{open}}$ for a given total energy E , that is,

$\tilde{S}^\dagger(E)\tilde{S}(E) = \mathbb{I}$ for all E , implying

$$\begin{aligned} \mathbf{r}(E)\mathbf{r}^\dagger(E) + \mathbf{t}(E)\mathbf{t}^\dagger(E) &= \mathbb{I} \\ \mathbf{r}(E)\mathbf{t}^\dagger(E) + \mathbf{t}(E)\mathbf{r}^\dagger(E) &= 0. \end{aligned} \quad (11)$$

The scattering map equation (7) determines the effect of a single collision on the system. If we now bombard the system with a stream of units, the evolution will be given by successive applications of the scattering map followed by the free evolution ruled by the Hamiltonian H_S [18]. If we neglect the free evolution, the behavior of the diagonal terms of the density matrix ρ_{JJ} , which are the populations of the energy levels $e_J = e_{j_U}^{(U)} + e_{j_S}^{(S)}$, is determined by the coefficients $\mathbb{S}_{J'J}^{JK}$ of the scattering map. Condition (8), particularized to $J' = K'$, indicates that these coefficients are different from zero only if $e_J = e_K$. Moreover, since the initial internal state of the unit is an eigenstate of H_U , $j_U = k_U$; hence, $e_{j_S}^{(S)} = e_{k_S}^{(S)}$. If the Hamiltonian of the system H_S is non degenerate, this implies $j_S = k_S$ and populations evolve independently of the off-diagonal terms of the density matrix

$$\rho'_{J'J} = \sum_J P_{J'J}(p_0)\rho_{JJ} \quad (12)$$

with the following transition probabilities that depend on the momentum p_0 of the incident unit:

$$P_{J'J}(p_0) \equiv \mathbb{S}_{J'J}^{JJ} = |t_{J'J}(E_{p_0} + e_J)|^2 + |r_{J'J}(E_{p_0} + e_J)|^2 \quad (13)$$

if $p_0^2 \geq 2m\Delta_{J'J}$ and zero otherwise. On the other hand, the unitarity of the scattering matrix on the subspace $\mathcal{H}_{\text{open}}$ of open channels, equation (11), implies that the off-diagonal terms decay [18], since $|t_{J'J}|^2 + |r_{J'J}|^2 \leq 1$, and that the trace of the density matrix is preserved, $\sum_{J'} P_{J'J}(p_0) = 1$ for all p_0 . From now on, we will focus on the effect of narrow wave packets and only discuss the behavior of the populations, assuming the off-diagonal terms of the density matrix rapidly decay due to the collisions.

2.3. Conditions for thermalization

In this subsection we explore whether the system thermalizes if the units are in equilibrium at inverse temperature β . This implies that the units are in an internal state $|s_{j_U}\rangle_U$ with probability

$$p_{j_U} = \frac{e^{-\beta e_{j_U}^{(U)}}}{Z_U} \quad (14)$$

where Z_U is the internal partition function of the unit. The momentum of the units coming from a thermal bath is distributed as [18, 19]:

$$\mu(p) = \frac{\beta|p|}{m} e^{-\beta p^2/(2m)} \quad p \in [0, \infty]. \quad (15)$$

This is the effusion distribution describing the momentum of particles in equilibrium that cross a given point or hit a fixed scatterer coming from the left (since our scatterer, as described by the total Hamiltonian (1), is symmetric, there is no need to explicitly consider the case of negative incident velocity). We have shown in reference [19] how this effusion distribution arises from the Maxwellian velocity distribution and a uniform density of classical particles, which characterize an ideal gas at equilibrium.

In this case, the populations $p(J) \equiv \rho_{JJ}$, obey the following evolution equation

$$p'(J') = \sum_J p(J)p(J \rightarrow J') \quad (16)$$

with

$$p(J \rightarrow J') = \int_0^\infty dp_0 \mu(p_0) P_{J'J}(p_0). \quad (17)$$

The evolution equation for the state of the system

$$p(j_S) = \sum_{j_U} p(j_S, j_U), \quad (18)$$

with $p(j_S, j_U) \equiv p(J)$, reads

$$p'(j'_S) = \sum_{j_S} p(j_S)p(j_S \rightarrow j'_S) \quad (19)$$

with

$$p(j_S \rightarrow j'_S) = \sum_{j_U, j'_U} \frac{e^{-\beta e_{j_U}^{(U)}}}{Z_U} p(J \rightarrow J') \quad (20)$$

where we recall that J denotes the pair of quantum numbers (j_S, j_U) .

A sufficient condition for thermalization is micro-reversibility or invariance of the collision probabilities under time reversal [18]. In a quantum system, the states are transformed under time reversal by means of an anti-unitary operator \mathbf{T} defined on the corresponding Hilbert space. Any anti-unitary operator can be written as $\mathbf{T} = \mathbf{C}U$, where \mathbf{C} is the conjugation of coordinates in a given basis and U is a unitary operator [22]. The time reversal operator depends on the physical nature of the system. Consider for instance a qubit with Hilbert space $\mathcal{H} = \mathbb{C}^2$. If the qubit is a 1/2 spin, then time-reversal must change the sign of all the components of the spin, i.e. $\mathbf{T}\sigma_\alpha\mathbf{T}^\dagger = -\sigma_\alpha$ for $\alpha = x, y, z$, where σ_α are the Pauli matrices. The anti-unitary operator that fulfills these transformations is $\mathbf{T} = \mathbf{C}\sigma_y$, where \mathbf{C} is the conjugation of the coordinates of the qubit in the canonical basis (the eigenbasis of σ_z) [22]. On the other hand, if the qubit is a two-level atom whose states are superpositions of real wave functions in the position representation, then the time reversal operator is just $\mathbf{T} = \mathbf{C}$, since the time-reversal of spinless particles is the conjugation of the wave function in the position representation.

In our case, the total time-reversal operator acting on the Hilbert space $\mathcal{H}_{U,p} \otimes \mathcal{H}_{U,int} \otimes \mathcal{H}_S$ can be decomposed into three parts $\mathbf{T} = \mathbf{T}_{U,p} \otimes \mathbf{T}_{U,int} \otimes \mathbf{T}_S$. The operator $\mathbf{T}_{U,p}$ is the conjugation of the spatial wave function of the unit in the position representation $\mathbf{T}_{U,p}\psi(x) = \psi^*(x)$, whereas in momentum representation reads $\mathbf{T}_{U,p}\phi(p) = \phi^*(-p)$ [22, 23]. The time-reversal operator for the internal degrees of freedom can in principle be any anti-unitary operator $\mathbf{T}_{int} = \mathbf{T}_{U,int} \otimes \mathbf{T}_S$.

Micro-reversibility occurs when the total Hamiltonian commutes with the time-reversal operator, $[H_{tot}, \mathbf{T}] = 0$. Since the kinetic part is already invariant under time reversal, the commutation $[H, \mathbf{T}_{int}] = 0$ is a sufficient condition for micro-reversibility. For simplicity, we further assume that $[H_0, \mathbf{T}_{int}] = 0$ and that the eigenstates of H_0 are time-reversal invariant: $\mathbf{T}_{int}|s_J\rangle = |s_J\rangle$ for all J . In appendix B we show that, if these conditions are fulfilled, then the scattering matrix obeys $\tilde{\mathbf{S}}^*\tilde{\mathbf{S}} = \mathbb{I}$. Combining this expression with the unitarity of $\tilde{\mathbf{S}}$, we conclude that the matrices \mathbf{t} and \mathbf{r} are symmetric for a given energy E :

$$\begin{aligned} \langle s_{J'} | \mathbf{t}(E) | s_J \rangle &= \langle s_J | \mathbf{t}(E) | s_{J'} \rangle \\ \langle s_{J'} | \mathbf{r}(E) | s_J \rangle &= \langle s_J | \mathbf{r}(E) | s_{J'} \rangle. \end{aligned} \quad (21)$$

If we now apply this symmetry to the transition probabilities given by equation (13), we obtain

$$P_{JJ'}(p_0) = P_{JJ'} \left(\sqrt{p_0^2 - 2m\Delta_{JJ'}} \right) \quad (22)$$

for all p_0 satisfying $p_0^2 \geq 2m\Delta_{JJ'}$.

Let us prove now that micro-reversibility, as expressed by equation (22) for the transition probabilities, is a sufficient condition for thermalization. We first focus on transitions of internal states including the unit, that is, from $|s_J\rangle$ to $|s_{J'}\rangle$. If $e_{J'} \geq e_J$, then $\Delta_{JJ'} \geq 0$ and the transition probability reads

$$p(J \rightarrow J') = \int_{\sqrt{2m\Delta_{JJ'}}}^{\infty} dp_0 \frac{\beta p_0}{m} e^{-\beta p_0^2/(2m)} P_{JJ'}(p_0). \quad (23)$$

Here, the lower limit in the integral is due to the fact that $P_{JJ'}(p_0)$ is zero for $p_0^2 \leq 2m\Delta_{JJ'}$. If we change the integration variable to $p'_0 = \sqrt{p_0^2 - 2m\Delta_{JJ'}} \Rightarrow dp'_0 = |p_0|dp_0/|p'_0|$, we obtain

$$p(J \rightarrow J') = \int_0^{\infty} dp'_0 \frac{\beta p'_0}{m} e^{-\beta(p_0'^2/(2m) + \Delta_{JJ'})} P_{JJ'} \left(\sqrt{p_0'^2 + 2m\Delta_{JJ'}} \right). \quad (24)$$

Finally, applying the micro-reversibility condition (22),

$$\begin{aligned} p(J \rightarrow J') &= e^{-\beta\Delta_{JJ'}} \int_0^{\infty} dp'_0 \frac{\beta p'_0}{m} e^{-\beta p_0'^2/(2m)} P_{JJ'}(p'_0) \\ &= e^{-\beta\Delta_{JJ'}} p(J' \rightarrow J). \end{aligned} \quad (25)$$

We can proceed in an analogous way for the case $e_{J'} \leq e_J$. The final result is the local detailed balance condition

$$\frac{p(J \rightarrow J')}{p(J' \rightarrow J)} = e^{-\beta(e_{J'} - e_J)} \quad \text{for all } J, J'. \quad (26)$$

We now explicitly consider the internal states of the unit. Recall that the subindex J in the previous sections comprises two quantum numbers $J = (j_S, j_U)$. If the internal states of the unit are in thermal equilibrium at inverse temperature β , then the transition probabilities between the states of the system are given by (20). The detailed balance condition (26) can be written as

$$p(J \rightarrow J') = e^{-\beta [e_{j'_U}^{(U)} + e_{j'_S}^{(S)} - e_{j_U}^{(U)} - e_{j_S}^{(S)}]} p(J' \rightarrow J). \quad (27)$$

Inserting (27) into (20), one gets

$$p(j_S \rightarrow j'_S) = e^{-\beta [e_{j'_S}^{(S)} - e_{j_S}^{(S)}]} p(j'_S \rightarrow j_S) \quad (28)$$

which is the detailed balance condition for the populations of the states of the system and ensures thermalization.

3. The transfer matrix method

We now go back to the calculation of the scattering matrix (10). In one dimension, a formal expression can be obtained using a transfer matrix approach [21]. This expression allows us to explore the consequences of different symmetries of the scattering problem as well as to derive approximations that preserve those symmetries.

3.1. Scattering states

The standard procedure to obtain the scattering matrix $\tilde{S}(E)$ for a given energy E consists in solving the time-independent Schrödinger equation

$$H_{\text{tot}}|\psi\rangle = \left[\frac{\hat{p}^2}{2m} + H_0 + \chi_L(\hat{x})H_{US} \right] |\psi\rangle = E|\psi\rangle \quad (29)$$

for quantum states $|\psi\rangle$ that behave as plane waves outside the scattering region $[-L/2, L/2]$. These solutions are called scattering states and are not proper quantum states since they are not normalizable. They can be written in terms of the eigenvectors of H_0 and H : $|s_J\rangle, |s'_J\rangle \in \mathcal{H}_{U,\text{int}} \otimes \mathcal{H}_S$, respectively (see equation (2)). In position representation, the scattering states, $\langle x|\psi\rangle \in \mathcal{H}_{U,\text{int}} \otimes \mathcal{H}_S$, read

$$\langle x|\psi\rangle = \begin{cases} \sum_J (\alpha_J e^{ik_J x} + \beta_J e^{-ik_J x}) |s_J\rangle & \text{for } x < -L/2 \\ \sum_J (\alpha'_J e^{ik'_J x} + \beta'_J e^{-ik'_J x}) |s'_J\rangle & \text{for } -L/2 < x < L/2 \\ \sum_J (\alpha''_J e^{ik_J x} + \beta''_J e^{-ik_J x}) |s_J\rangle & \text{for } L/2 < x. \end{cases} \quad (30)$$

Inserting this wave function into the Schrödinger equation (29), one obtains the following energy conservation condition for the wave vectors k_J and k'_J :

$$\frac{k_J^2}{2m} + e_J = \frac{k_J'^2}{2m} + e'_J = E \quad \text{for all } J. \quad (31)$$

This condition fixes the value of the wave vectors k_J and k'_J , which can be real or imaginary depending on the energy E . An imaginary wave vector k_J implies an exponential decay outside the scattering region, which does not describe a scattering event. This is why the scattering matrix is defined only for states $|s_J\rangle$ with real k_J , which span the subspace of open channels $\mathcal{H}_{\text{open}}$ for a given energy E , introduced in equation (9). On the other hand, k'_J can be real or imaginary, the latter case corresponding to channels where the transmission is due to quantum tunneling.

3.2. Transfer and scattering matrices

The amplitudes of the scattering state (30) in the different segments of the real line, $\alpha_J, \beta_J, \alpha'_J, \beta'_J, \alpha''_J$, and β''_J , are determined by imposing the continuity and differentiability of the wave function at $x = -L/2$ and

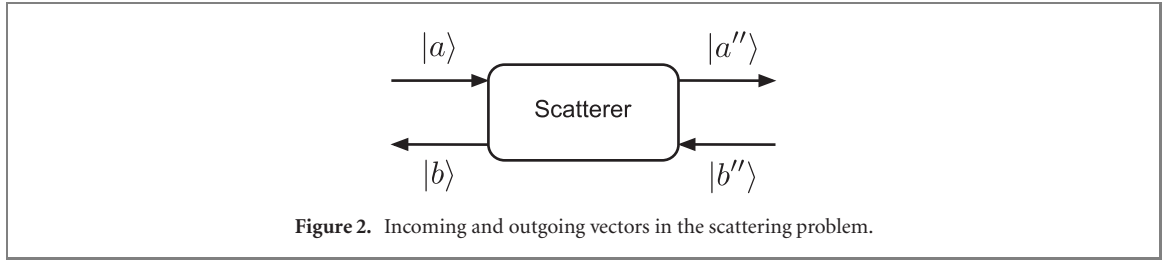


Figure 2. Incoming and outgoing vectors in the scattering problem.

$x = L/2$. It is convenient to write the amplitudes as coordinates of vectors in the internal Hilbert space $\mathcal{H}_{U,\text{int}} \otimes \mathcal{H}_S$:

$$\begin{aligned} |a\rangle &= \sum_J \alpha_J |s_J\rangle; & |a'\rangle &= \sum_J \alpha'_J |s'_J\rangle; & |a''\rangle &= \sum_J \alpha''_J |s_J\rangle \\ |b\rangle &= \sum_J \beta_J |s_J\rangle; & |b'\rangle &= \sum_J \beta'_J |s'_J\rangle; & |b''\rangle &= \sum_J \beta''_J |s_J\rangle. \end{aligned} \quad (32)$$

We also introduce two operators, acting on the internal Hilbert space $\mathcal{H}_{U,\text{int}} \otimes \mathcal{H}_S$, which will play an important role in the rest of the paper:

$$\mathbb{K}_0(E) \equiv \sqrt{2m(E - H_0)} \mathbb{K}(E) \equiv \sqrt{2m(E - H)}. \quad (33)$$

We call them WVOs, since their eigenvalues are the wave vectors corresponding to a given energy E : $\mathbb{K}_0(E)|s_J\rangle = k_J|s_J\rangle$ and $\mathbb{K}(E)|s'_J\rangle = k'_J|s'_J\rangle$. Notice that they are self-adjoint only for sufficiently high energy. In particular, \mathbb{K}_0 is self-adjoint when restricted to $\mathcal{H}_{\text{open}}$.

The boundary conditions allow us to eliminate the intermediate amplitudes $|a'\rangle$ and $|b'\rangle$ and find a relationship between the rest. The relationship can be written as

$$\begin{pmatrix} |a''\rangle \\ |b''\rangle \end{pmatrix} = \mathcal{M} \begin{pmatrix} |a\rangle \\ |b\rangle \end{pmatrix}. \quad (34)$$

\mathcal{M} is called the transfer matrix and connects the amplitudes of the plane waves at the right and at the left sides of the scatterer (see figure 2). Notice that it is a matrix defined in the Hilbert space $[\mathcal{H}_{U,\text{int}} \otimes \mathcal{H}_S] \oplus [\mathcal{H}_{U,\text{int}} \otimes \mathcal{H}_S]$. In appendix A, we obtain the following closed expression for the transfer matrix from the boundary conditions:

$$\mathcal{M} = \mathbb{M}^{-1}(L/2, \mathbb{K}_0) \mathbb{M}(L/2, \mathbb{K}) \mathbb{M}^{-1}(-L/2, \mathbb{K}) \mathbb{M}(-L/2, \mathbb{K}_0), \quad (35)$$

where we have introduced the matrix $\mathbb{M}(x, \mathbb{K})$ acting on the Hilbert space $[\mathcal{H}_{U,\text{int}} \otimes \mathcal{H}_S] \oplus [\mathcal{H}_{U,\text{int}} \otimes \mathcal{H}_S]$ and depending on a position x and an operator \mathbb{K} :

$$\mathbb{M}(x, \mathbb{K}) \equiv \begin{pmatrix} e^{i\mathbb{K}x} & e^{-i\mathbb{K}x} \\ \mathbb{K} e^{i\mathbb{K}x} & -\mathbb{K} e^{-i\mathbb{K}x} \end{pmatrix}. \quad (36)$$

An alternative way of relating the amplitudes of the plane waves is the matrix \mathcal{S} connecting the incoming and outgoing amplitudes (see figure 2):

$$\begin{pmatrix} |b\rangle \\ |a''\rangle \end{pmatrix} = \mathcal{S} \begin{pmatrix} |a\rangle \\ |b''\rangle \end{pmatrix} = \begin{pmatrix} \mathcal{S}_{11}|a\rangle + \mathcal{S}_{12}|b''\rangle \\ \mathcal{S}_{21}|a\rangle + \mathcal{S}_{22}|b''\rangle \end{pmatrix}. \quad (37)$$

A direct comparison between (34) and (37) yields [21]:

$$\begin{aligned} \mathcal{S}_{11} &= -\mathcal{M}_{22}^{-1} \mathcal{M}_{21} & \mathcal{S}_{12} &= \mathcal{M}_{22}^{-1} \\ \mathcal{S}_{21} &= \mathcal{M}_{11} - \mathcal{M}_{12} \mathcal{M}_{22}^{-1} \mathcal{M}_{21} & \mathcal{S}_{22} &= \mathcal{M}_{12} \mathcal{M}_{22}^{-1}. \end{aligned} \quad (38)$$

The matrix \mathcal{S} is not exactly the scattering matrix $\tilde{\mathcal{S}}(E)$, defined in equation (10), for two reasons. First, \mathcal{S} acts on the whole Hilbert space $[\mathcal{H}_{U,\text{int}} \otimes \mathcal{H}_S] \oplus [\mathcal{H}_{U,\text{int}} \otimes \mathcal{H}_S]$, whereas the scattering matrix $\tilde{\mathcal{S}}$ introduced in equation (10) is restricted to the space open channels, $\mathcal{H}_{\text{open}}$, spanned by the eigenstates with real wave vectors k_J . Second, the entries of $\tilde{\mathcal{S}}$ are the transmission and reflection amplitudes, which are given respectively by the amplitudes of the transmitted and reflected waves multiplied by the ratio of

outgoing to incoming momenta [18, 23]. According to equation (10), the scattering matrix can be written as the following operator acting on $\mathcal{H}_{\text{open}} \oplus \mathcal{H}_{\text{open}}$:

$$\tilde{\mathcal{S}} \equiv \begin{pmatrix} \mathbb{K}_0^{1/2} & 0 \\ 0 & \mathbb{K}_0^{1/2} \end{pmatrix} \mathcal{S} \begin{pmatrix} \mathbb{K}_0^{-1/2} & 0 \\ 0 & \mathbb{K}_0^{-1/2} \end{pmatrix} = \mathbb{K}_0^{1/2} \mathcal{S} \mathbb{K}_0^{-1/2} \quad (39)$$

where all the operators \mathbb{K}_0 and \mathcal{S}_{ij} are restricted to $\mathcal{H}_{\text{open}}$.

3.3. High-energy limit

The matrix \mathcal{M} can be calculated exactly from equation (35). However, here we introduce an approximation that preserves the symmetries and the unitarity of the scattering matrix and therefore provides a simple implementation of a thermal reservoir. The approximation is valid for incident particles with large kinetic energy. More precisely, if $E \gg e_j, e'_j$, all the wave vectors are approximately equal, $k_j \simeq k'_j \simeq \sqrt{2mE}$, and we can approximate $\mathbb{K}^{-1}\mathbb{K}_0 \simeq \mathbb{I}$ yielding (see appendix C for a detailed calculation)

$$\mathcal{M} \simeq \begin{pmatrix} e^{-i\mathbb{K}_0 L/2} e^{i\mathbb{K}L} e^{-i\mathbb{K}_0 L/2} & 0 \\ 0 & e^{i\mathbb{K}_0 L/2} e^{-i\mathbb{K}L} e^{i\mathbb{K}_0 L/2} \end{pmatrix}. \quad (40)$$

Using equation (38) and the definition of the scattering matrix (39), we find that the scattering matrix $\tilde{\mathcal{S}}$ and the matrix \mathcal{S} in this approximation are

$$\tilde{\mathcal{S}} \simeq \mathcal{S} \simeq \begin{pmatrix} 0 & e^{-i\mathbb{K}_0 L/2} e^{i\mathbb{K}L} e^{-i\mathbb{K}_0 L/2} \\ e^{-i\mathbb{K}_0 L/2} e^{i\mathbb{K}L} e^{-i\mathbb{K}_0 L/2} & 0 \end{pmatrix}. \quad (41)$$

We see that, in this approximation, the reflection amplitudes vanish and the transition amplitudes read

$$\langle s_{j'} | \mathbf{t} | s_j \rangle \simeq e^{-i(k_j + k_{j'})L/2} \langle s_{j'} | e^{i\mathbb{K}L} | s_j \rangle. \quad (42)$$

This matrix \mathcal{S} is unitary and symmetric for a given energy $E = k_j^2/(2m) + e_j = k_{j'}^2/(2m) + e_{j'}$ if \mathbb{K} is self-adjoint, that is, if all k'_j are real. This occurs if the total energy E is larger than the maximum eigenvalue of H . Hence, for sufficiently high incident kinetic energy, this approximation fulfills all the symmetries of the original collision problem. To see that the matrix is symmetric, notice that $[H, \mathbf{T}_{\text{int}}] = 0$ implies $e^{i\mathbb{K}L} \mathbf{T}_{\text{int}} = \mathbf{T}_{\text{int}} e^{-i\mathbb{K}L}$ in the subspace where \mathbb{K} is self-adjoint. Therefore, for energies E larger than the maximum eigenvalue of H , we have

$$\begin{aligned} \langle s_{j'} | e^{i\mathbb{K}L} | s_j \rangle &= (\mathbf{T}_{\text{int}} | s_{j'} \rangle, e^{i\mathbb{K}L} \mathbf{T}_{\text{int}} | s_j \rangle) = (\mathbf{T}_{\text{int}} | s_{j'} \rangle, \mathbf{T}_{\text{int}} e^{-i\mathbb{K}L} | s_j \rangle) \\ &= (| s_{j'} \rangle, e^{-i\mathbb{K}L} | s_j \rangle)^* = \langle s_{j'} | e^{-i\mathbb{K}L} | s_j \rangle^* \\ &= \langle s_j | e^{i\mathbb{K}L} | s_{j'} \rangle. \end{aligned} \quad (43)$$

Here (\cdot, \cdot) is the scalar product in the Hilbert space and we have used the time-reversal invariance of the eigenstates of H_0 , $\mathbf{T}_{\text{int}} | s_j \rangle = | s_j \rangle$ for all j , and that any anti-unitary operator verifies $(\mathbf{T} | a \rangle, \mathbf{T} | b \rangle) = (| a \rangle, | b \rangle)^*$. Notice that the same symmetry holds if we replace $\mathbb{K}L$ by any real function of H .

4. Collisional thermostats

We now build two simple models of thermostats based on the approximation derived in the previous section. The first one is a direct application of equation (42), where the entries of the scattering matrix are given in terms of the WVO \mathbb{K} . The second one is a further approximation obtained by a Taylor expansion of the WVOs (33). The resulting expression for the transmission amplitudes is given in terms of the total internal Hamiltonian H and resembles the repeated-interaction scheme with an interaction time that depends on the total energy.

4.1. Wave-vector-operator model

Equation (42) is a valid approximation for high incident kinetic energy. To complete our first thermostat model, we need an expression for the transmission and reflection amplitudes at low velocities. In order to preserve micro-reversibility and the unitarity of the scattering matrix, we adopt the simplest assumption for low energies, namely, that the incident unit is reflected without affecting the state of the system. This is also justified by the fact that in a large scatterer the transmission amplitudes corresponding to tunneling vanish. However, from the point of view of the system, it does not matter whether the unit is reflected or transmitted, as long as it does not affect the system. Then, for simplicity, we define our model of a

collisional thermostat as given by vanishing reflection amplitudes, $r_{J'J}(E) = 0$ for all E , and the following transmission amplitudes:

$$t_{J'J}(E) = \begin{cases} e^{-iL(k_J+k_{J'})/2} \langle s_{J'} | e^{iL\mathbb{K}(E)} | s_J \rangle & \text{if } E > e_{\max} \\ \delta_{J'J} & \text{if } E \leq e_{\max} \end{cases} \quad (44)$$

where $E = p_0^2/(2m) + e_J$ and e_{\max} is the maximum of the eigenvalues of H and H_0 . With this choice

$$\sum_{J'} [|t_{J'J}(E)|^2 + |r_{J'J}(E)|^2] = 1 \quad (45)$$

for all J and E , ensuring the conservation of the trace of the density matrix $\text{Tr}(\rho') = \text{Tr}(\rho)$.

The transmission amplitudes defined by equation (44) obey condition (21), as shown in the previous section 3.3. We conclude that our model, based on the WVO \mathbb{K} , induces the thermalization of the system. Consequently, it constitutes a simple model of a thermostat. Furthermore, it is also a good approximation of a system colliding with units that escape from a thermal reservoir, specially for large scatterers. In section 5, we check the validity of this approximation in explicit examples.

4.2. Random-interaction-time model

We now present a second model that also induces thermalization and is more directly related to the repeated interaction schemes considered in the literature [11, 13], where the interaction H_{US} is switched on for a time interval. This can be done if the incident momentum is large and we can further expand the operator $\mathbb{K}(E) = \sqrt{2m(E-H)}$ as

$$\mathbb{K}(E) \simeq \sqrt{2mE} - \sqrt{\frac{m}{2E}} H. \quad (46)$$

An analogous expansion of the wave vectors outside the scattering region yields $k_J \simeq \sqrt{2mE} - e_J \sqrt{m/(2E)}$. Inserting these expressions in the transmission amplitudes given by equation (42), we get

$$t_{J'J}(E) \simeq e^{i\tau(E)[e_{J'}+e_J]/2} \langle s_{J'} | e^{-i\tau(E)H} | s_J \rangle. \quad (47)$$

Here, we have introduced the time

$$\tau(E) \equiv \frac{L}{v_E} = \frac{L}{\sqrt{2E/m}}, \quad (48)$$

which is the time a classical particle with velocity $v_E \equiv \sqrt{2E/m} = \sqrt{(p_0/m)^2 + 2e_J/m}$ takes to cross the scattering region of length L . Except for a phase, equation (47) is equivalent to the evolution of the state $|s_J\rangle$ under the total internal Hamiltonian $H = H_0 + H_{US}$ during a time $\tau(E)$, which is, approximately, the interaction time between the wave packet and the scatterer. We thus recover for the transmission amplitudes the usual picture that ignores the translational part of the unit and considers that the coupling is switched on for a given time $\tau(E)$ [11, 13]. Notice however that this velocity does not exactly coincide with the velocity of the wave packet $v_{\text{packet}} \equiv p_0/m$. In fact, the scattering matrix resulting from setting the interaction time equal to $\tau_{\text{packet}} \equiv L/v_{\text{packet}} = Lm/p_0$ does not obey micro-reversibility and does not thermalize the system, as we show in section 5 for an specific example.

Two important remarks must be made. First, expression (47) can be evaluated for any pair of states, J and J' , and any positive energy E . However, the transfer matrix is only defined for open channels, obeying $E \geq e_J, e_{J'}$. To preserve the unitarity of the scattering matrix we have to restrict the use of (47) to energies E larger than the eigenvalues of H_0 . To be consistent with the wave-vector-operator (WVO) model, we adopt here a more conservative strategy, restricting expression (47) to energies higher than e_{\max} , the maximum eigenvalue of both H_0 and H . We also assume that e_{\max} is positive, to avoid a negative total energy E , which would yield an imaginary velocity v_E . Summarizing, our model consists of null reflection amplitudes, $r_{J'J}(E) = 0$ for all E , and transmission amplitudes given by

$$t_{J'J}(E) = \begin{cases} e^{i\tau(E)[e_{J'}+e_J]/2} \langle s_{J'} | e^{-i\tau(E)H} | s_J \rangle & \text{if } E > e_{\max} \\ \delta_{J'J} & \text{if } E \leq e_{\max}. \end{cases} \quad (49)$$

With this definition, our random-interaction-time (RIT) model, like the WVO model, preserves all the properties of the exact scattering matrix and consequently induces the thermalization of the system. As in the previous model, we have set to zero the reflection amplitudes for $E \leq e_{\max}$, although for low energies the unit is most likely reflected. The choice in (49) is equivalent to assume that the system is not affected if $E \leq e_{\max}$, independently of whether the unit is reflected or transmitted.

The second remark is to notice that the interaction time $\tau(E)$ depends on the zero of the total energy, that is, if we add a constant E_0 to the total Hamiltonian H_{tot} , $\tau(E)$ changes. Then the transition amplitudes will depend as well on the zero of energy. The reason of this dependency is the Taylor expansion around $H = 0$ in equation (46). Shifting the internal energies an amount E_0 is equivalent to expanding the square root around $H = -E_0$ in equation (46). Hence, to minimize the error in the expansion we have to choose the zero of energy in such a way that H is small. There are several criteria to define the ‘smallness’ of an operator, based on different matrix norms. For the example in section 5, we minimize the spectral norm of H , which is the square root of the largest eigenvalue of $H^\dagger H = H^2$. Notice however that all the models obtained by an energy shift with $e_{\text{max}} > 0$ are effective thermostats when the scatterer is bombarded by equilibrium units, since equation (49) is unitary and fulfills micro-reversibility.

The model given by equation (49) and the corresponding scattering map in equation (7) are similar to the ones previously considered in the literature [11, 13], except for the randomization of the interaction time $\tau(E)$, which depends on the initial state $|s_j\rangle$, and for the removal of coherences due to tracing out the outgoing narrow packets [18].

4.3. Kraus representation

To further explore the differences and similarities between our thermostats and a repeated-interaction reservoir, it is convenient to use the Kraus representation of the scattering map given by equation (5), together with (7) and condition (8). If we neglect the reflecting amplitudes, a representation of this map is given by the following Kraus operators:

$$M_l = \sum_{JJ'} t_{JJ'}(E_{p_0} + e_j) \delta_{\Delta_{J'}, \Delta_l} |s_{J'}\rangle \langle s_J| \quad (50)$$

where δ is a Kronecker delta and Δ_l runs over all possible Bohr frequencies of the free internal Hamiltonian H_0 . Indeed, the map

$$\rho' = \sum_l M_l \rho M_l^\dagger \quad (51)$$

in the eigenbasis of H_0 is given by the tensor

$$\mathbb{S}_{JJ'}^{KK'} = \sum_l \langle s_{J'} | M_l | s_J \rangle \langle s_K | M_l^\dagger | s_{K'} \rangle, \quad (52)$$

which coincides with the one given by equations (5), (7) and (8), if the reflection amplitudes are neglected. If we now use the approximation (49), the Kraus operators in the eigenbasis of H_0 read

$$\langle s_{J'} | M_l | s_J \rangle = e^{-i\tau(E)(e_j + e_{j'})/2} \langle s_{J'} | e^{-i\tau(E)H} | s_J \rangle \delta_{\Delta_{J'}, \Delta_l} \quad (53)$$

with $E = p_0^2/(2m) + e_j$.

On the other hand, the Kraus representation of the unitary evolution in a repeated-interaction scheme consists of a unique unitary operator M given by

$$\langle s_{J'} | M | s_J \rangle = \langle s_{J'} | e^{-i\tau_{\text{int}} H} | s_J \rangle \quad (54)$$

where τ_{int} is the interaction time. Comparing (53) and (54), we see three main differences: first, the Kronecker delta kills all coherences between jumps with different Bohr frequencies. Recall that the map acting on a pure state can be seen as the application of a randomly chosen operator M_l [24]. The Kronecker delta only allows for superpositions with the same energy jump Δ_l . This is a consequence of using narrow packets, which is a necessary condition for thermalization, as proved in reference [18]. Remarkably, this condition has also been shown to be necessary to derive a fluctuation theorem for quantum maps (see equation (12) in reference [24]), and is equivalent to imposing that the energy exchange with the reservoir, i.e. the heat, is well defined for each possible transformation of a pure state given by the Kraus operators. This implies that heat is well defined for any quantum stochastic trajectory [24]. Second, the interaction time in the RIT model, $\tau(E)$, depends on the energy of the initial state e_j . Third, there is an extra phase that appears in the solution of the scattering problem, although it does not play a role in thermalization.

5. An example

In this section we analyze in detail an explicit example where the units and the system are single qubits. We consider the following free Hamiltonian and interaction term between the system and the internal state of

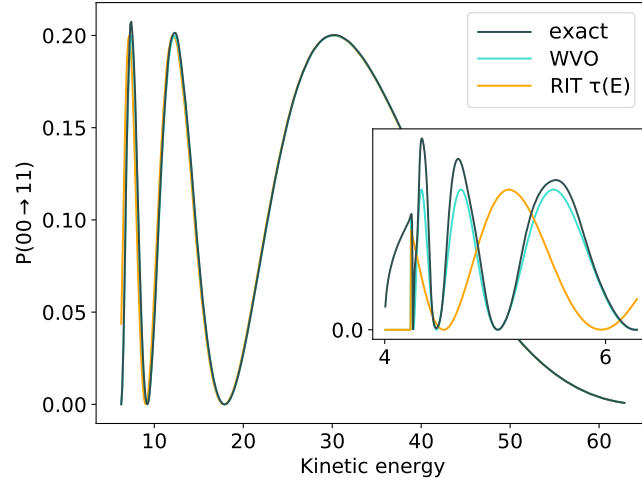


Figure 3. Probability of the transition $|00\rangle_{US} \rightarrow |11\rangle_{US}$ for $J_x = 1$, $J_y = 0$, $\omega_S = \omega_U = 1$, $m = 0.1$, and $L = 50$. We show the exact result obtained from the transfer matrix equation (35) (dark green), the wave-vector-operator model (WVO, light green) given by equation (44), the random-interaction-time model (RIT, orange) given by equation (49). The inset shows the behavior for low kinetic energy, where one can see that the WVO model still reproduces rather well the exact probabilities. Below $e_{\max} = 2.23$ the transition probability vanishes for the two models, WVO and RIT.

the unit:

$$H_0 = \omega_U \sigma_z^U \otimes \mathbb{I} + \omega_S \mathbb{I} \otimes \sigma_z^S \quad (55)$$

$$H_{US} = J_x \sigma_x^U \otimes \sigma_x^S + J_y \sigma_y^U \otimes \sigma_y^S, \quad (56)$$

where $\sigma_i^{U,S}$ are the Pauli matrices in the Hilbert space of the unit and the system, respectively, $2\omega_{U,S}$ is the level spacing of each qubit, and $J_{x,y}$ are coupling constants. The eigenstates of the free Hamiltonian H_0 are $|00\rangle_{US}$, $|01\rangle_{US}$, $|10\rangle_{US}$, and $|11\rangle_{US}$ with energies $\omega_U + \omega_S$, $\omega_U - \omega_S$, $-\omega_U + \omega_S$, and $-\omega_U - \omega_S$, respectively. This system has been exhaustively studied in reference [13] in the context of the repeated-interaction coupling mediated by an external agent.

The system obeys the conditions for thermalization discussed in section 2.3. First, $H_S = \omega_S \sigma_z^S$ has no degenerate levels and no Bohr degeneracies (notice that the global internal Hamiltonian H_0 does exhibit degeneracies and Bohr degeneracies, specially if $\omega_U = \omega_S$; however, as discussed above equation (12), the only condition for thermalization is that the system Hamiltonian H_S is non-degenerate, since the internal state of the incident units is disentangled from the system and at equilibrium with respect to H_U). Second, if we take as time-reversal operator $\mathbf{T}_{\text{int}} = C$, where C the conjugation of coordinates in the canonical basis, then $\mathbf{T}_{\text{int}}^\dagger \sigma_y^{U,S} \mathbf{T}_{\text{int}} = -\sigma_y^{U,S}$, $\mathbf{T}_{\text{int}}^\dagger \sigma_x^{U,S} \mathbf{T}_{\text{int}} = \sigma_x^{U,S}$, and $\mathbf{T}_{\text{int}}^\dagger \sigma_z^{U,S} \mathbf{T}_{\text{int}} = \sigma_z^{U,S}$, hence $[H, \mathbf{T}_{\text{int}}] = [H_0, \mathbf{T}_{\text{int}}] = 0$ and micro-reversibility is fulfilled. Furthermore, the eigenstates of H_0 are invariant under time reversal, $\mathbf{T}_{\text{int}}|e_J\rangle = |e_J\rangle$ for all J (notice that this is not the time reversal operator of a spin 1/2; it is however an admissible time reversal operator for a qubit, as discussed in section 2.3). Consequently, if the system is bombarded by narrow wave packets at equilibrium, the scattering map drives the system towards the equilibrium state, and this thermalization occurs for the exact scattering map as well as for any of the two effective models introduced in the previous section.

5.1. Transition probabilities

We first check whether the two models presented in the previous section are able to reproduce the transition probabilities $P_{JJ}(p_0)$. We calculate the transfer matrix given by equation (35) and compare the exact transition probabilities in equation (13) for a given incident momentum p_0 with the ones obtained from the WVO model, equation (44), and the random interaction model (RIT), equation (49). The comparison is shown in figure 3 as a function of the kinetic energy $p_0/(2m)$, for the transition $|00\rangle_{US} \rightarrow |11\rangle_{US}$. As expected, the two models reproduce with good accuracy the exact transition probabilities for high kinetic energy. It is remarkable that the wave vector operator model is a very good approximation of the scattering problem even for low kinetic energy, as shown in the inset, whereas the RIT model fails in this regime.

5.2. Thermalization

We now bombard the qubit with narrow wave packets with random momentum, according to the effusion distribution at temperature T , and a random internal state, according to the Boltzmann distribution at the

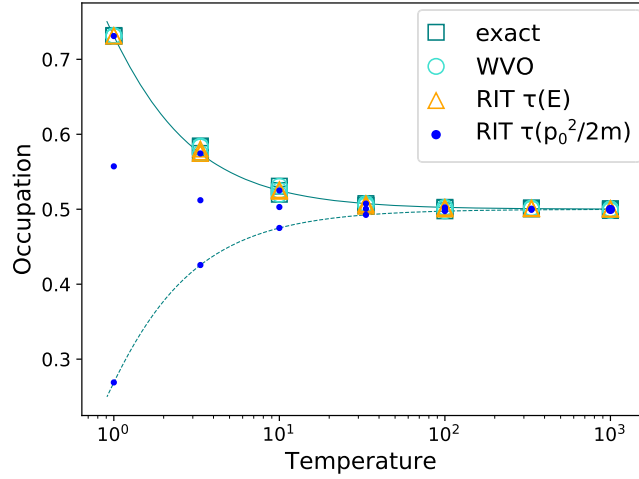


Figure 4. Stationary population of the ground state of the qubit for $J_y = 1, 0, -1$, $J_x = 1$ and $\omega_S = \omega_U = 1$, $m = 0.1$, and $L = 50$. We depict the exact solution of the scattering problem using the transfer matrix (35) (dark green squares) and the populations given by different models: the WVO model given by equation (44) (green circles) and the RIT model given by equation (49) (orange triangles). The exact solution and the two models induce thermalization at the same temperature as the bath, as expected. We also show the population if the interaction time is chosen as $\tau_{\text{packet}} \equiv \tau(p_0^2/(2m)) = Lm/p_0$ (dark blue dots, $J_y = 1, 0, -1$ from top to bottom), which clearly departs from the thermal state and even exhibits negative absolute temperatures or population inversion for $J_y = -J_x = -1$ (see appendix D for an analytical proof of this result). The continuous and dashed light green curves depict the population of the fundamental level in the canonical ensemble with positive and negative temperature respectively.

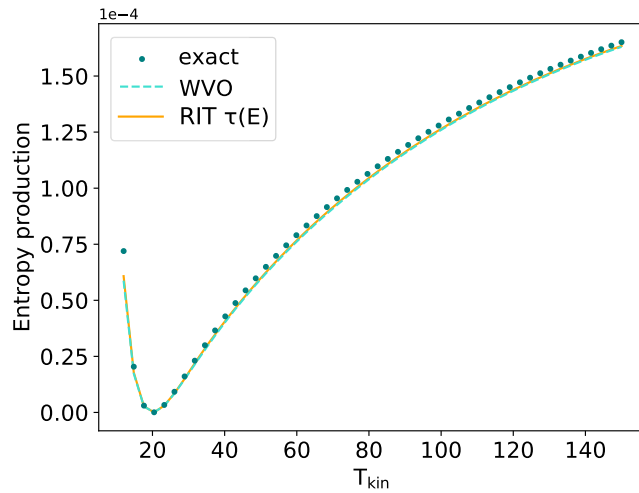


Figure 5. Entropy production per collision as a function of the temperature of the kinetic degrees of freedom, T_{kin} , for $J_x = 1$, $J_y = 0$, $\omega_U = \omega_S = 1$, $m = 1$, $L = 50$ and a temperature $T_{\text{int}} = 20$ of the internal degrees of freedom of the units. We compare the exact (numerical) solution of the scattering problem using the transfer matrix (35), the WVO model and the RIT model.

same temperature. We simulate 500 quantum trajectories where the system jumps between pure eigenstates of the Hamiltonian H_S , and calculate the steady population of the two levels of the qubit. Each trajectory is 10 000 collision long, providing sufficient statistics to neglect the uncertainty.

As expected, the system thermalizes not only for the exact solution of the scattering problem, given by equation (35), but also for the two models, equation (44) and (49). In figure 4, we plot the stationary population of the ground state in the three cases and in the thermal state.

To stress the importance of micro-reversibility for thermalization, we also plot in the figure with dark blue circles the population when the interaction time is chosen as $\tau_{\text{packet}} \equiv \tau(p_0^2/(2m)) = L/v_{\text{packet}}$, where $v_{\text{packet}} = p_0/m$ is the velocity of the incoming wave packet. In this case, the system does not reach the temperature of the reservoir and can even exhibit population inversion (see appendix D for a detailed discussion of the model and reference [25] for a general discussion of the phenomenon within the repeated interaction framework). From the point of view of the dynamics of the system, it is striking that the replacement of $v_E = \sqrt{2E/m}$ by $v_{\text{packet}} = p_0/m$ in the calculation of the interaction time has such

significant consequences. Notice however that the interaction time in the RIT model with time given by equation (48) depends both on the energy of the system $e_{js}^{(S)}$ and of the internal state of the unit $e_{ju}^{(U)}$.

5.3. Non-equilibrium

Finally, we check the two models in a non-equilibrium scenario where the internal states of the unit are in equilibrium at temperature T_{int} , different from the temperature T_{kin} of the effusion distribution, i.e. the state of the unit is given by (14) and (15) but with temperatures T_{int} and T_{kin} , respectively. In this situation, the system is exchanging heat with two different thermal baths and reaches a non-equilibrium steady state where a heat Q is transferred from the hot to the cold bath in each collision. In our case, the two baths are the internal and the kinetic degrees of freedom of the unit. The irreversible heat transfer induces an entropy production per collision $\Delta S = Q|1/T_{\text{int}} - 1/T_{\text{kin}}|$, which is shown in figure 5 as a function of the kinetic temperature T_{kin} , for a fixed internal temperature $T_{\text{int}} = 20$ and for the two different models and the exact solution of the scattering matrix. In this simulation, the heat Q is calculated as minus the change of the internal energy of the unit in each collision, which is then averaged over quantum trajectories in the steady state. We see in the figure that, for this range of temperatures, the two thermostats are accurate approximations of the exact solution of the scattering problem, even far from equilibrium.

6. Conclusions

We have presented two heuristic models of collisional thermostats that induce thermalization. Our models are relatively simple to implement numerically and analytically, and overcome the main drawback of previous repeated-interaction schemes that do not induce thermalization due to the energy introduced when switching on and off the interaction [10, 11, 13]. Moreover, the two thermostats are good approximations to the scattering problem even in situations far from equilibrium, as shown in section 5.

Besides the practical interest of our models as tools to simulate or study analytically the behavior of quantum systems in contact with one or several thermal baths, they are also related to a fundamental issue in thermodynamics: the nature of heat and work.

The RIT model is similar to the repeated-interaction reservoirs considered in the literature [11, 13]. We have explored the differences between both schemes in sections 4.2 and 4.3. The main ones are the removal of coherences resulting from jumps with different energy and that the interaction time is random. Both differences make the energy transferred from the reservoir to the system to be heat instead of work. Notice also that populations thermalize for a very specific distribution of interaction times—the one resulting from the effusion distribution and fulfilling the micro-reversibility condition. This result raises the question of which are the conditions or signatures for an energy transfer to be considered as heat. Heat is defined as an energy transfer between a system and its surroundings inducing a change of entropy in the latter. The definition is precise and unambiguous if the environment is at equilibrium. The distinction between heat and work is also determinant for the performance of thermal machines: work ‘can do more’ than heat. Since a transfer of heat Q from a thermal bath at temperature T is accompanied by a decrease of entropy $\Delta S_{\text{bath}} = -Q/T$ in the bath, the second law implies that either Q is negative or there must be an increase of entropy in the system or a dissipation of heat into another bath to compensate ΔS_{bath} . In other words, not all the extracted heat can be transformed into useful work.

Hence, we can identify an energy transfer as heat by analyzing either where this energy comes from or what it can do. In most situations, the first option is the easiest to follow: by knowing where the energy comes from we can infer what it can do. This is one of the main achievements of classical thermodynamics.

However, if we do not have information about the physical nature or the state of the environment and know only the statistical properties of the energy transfer, how can we split it into heat and work? Our models shed some light into this problem. First, heat destroys certain coherences. Second, the random interaction times must follow a very specific distribution. If one uses a distribution different from effusion [19] or if, for instance, the interaction time is calculated using the incident velocity p_0/m instead of the one given by equation (48), thermalization fails, as shown in figure 4. This implies that part of the energy exchanged can be considered as work, since, if the system does not thermalize, it would be possible to create a thermal machine able to extract energy from a single thermal bath, even with classical systems [19].

To summarize, we have presented two simple models of collisional thermostats given by equations (44) and (47), which are novel tools to analyze open quantum systems. The models involve the removal of coherences resulting from jumps with different energy transfers between the system and the reservoir, allowing to interpret the energy exchange as heat. These results help to address the problem of how to split a given random transfer of energy into heat and work, a fundamental open question with practical implications. Its solution could be useful even for classical, meso- and macro-scopic systems, since it will help to establish benchmarks for energy harvesting from fluctuations.

Acknowledgments

SLJ is supported by the Doctoral Training Unit on Materials for Sensing and Energy Harvesting (MASSENA) with the Grant: FNR PRIDE/15/10935404. ME acknowledges financial support from the European Research Council (project NanoThermo, ERC-2015-CoG Agreement No. 681456) and the FQXi foundation, project ‘Information as a fuel in colloids and superconducting quantum circuits’ (FQXi-IAF19-05). FB thanks Fondecyt project 1191441 and the Millennium Nucleus ‘Physics of active matter’ of ANID (Chile). Part of this work was conducted at the KITP, a facility supported by the US National Science Foundation under Grant No. NSF PHY-1748958. JMRP, JT and IL acknowledge financial support from the Spanish Government (Grant Contracts FIS-2017-83706-R and PID2020-113455GB-I00) and from the Foundational Questions Institute Fund, a donor advised fund of Silicon Valley Community Foundation (Grant Number FQXi-IAF19-01).

Data availability statement

All data that support the findings of this study are included within the article (and any supplementary files).

Appendix A. Transfer and scattering matrices

The coefficients α_J , β_J , etc in equation (30) are determined by imposing the continuity of the wave function and its first derivative at the boundaries of the scattering regions $[-L/2, L/2]$. At $x = -L/2$:

$$\sum_J \left(\alpha_J e^{-ik_J L/2} + \beta_J e^{ik_J L/2} \right) |s_J\rangle = \sum_J \left(\alpha'_J e^{-ik'_J L/2} + \beta'_J e^{ik'_J L/2} \right) |s'_J\rangle \quad (\text{A1})$$

$$\sum_J k_J \left(\alpha_J e^{-ik_J L/2} - \beta_J e^{ik_J L/2} \right) |s_J\rangle = \sum_J k'_J \left(\alpha'_J e^{-ik'_J L/2} - \beta'_J e^{ik'_J L/2} \right) |s'_J\rangle, \quad (\text{A2})$$

and, at $x = L/2$:

$$\sum_J \left(\alpha''_J e^{ik_J L/2} + \beta''_J e^{-ik_J L/2} \right) |s_J\rangle = \sum_J \left(\alpha'_J e^{ik'_J L/2} + \beta'_J e^{-ik'_J L/2} \right) |s'_J\rangle \quad (\text{A3})$$

$$\sum_J k_J \left(\alpha''_J e^{ik_J L/2} - \beta''_J e^{-ik_J L/2} \right) |s_J\rangle = \sum_J k'_J \left(\alpha'_J e^{ik'_J L/2} - \beta'_J e^{-ik'_J L/2} \right) |s'_J\rangle. \quad (\text{A4})$$

These equations can be written in a more compact form using the WVOs (33), the vectors defined in (32), and the matrix $\mathbb{M}(x, \mathbb{K})$ defined in (36). We recall the form of this matrix, which depends on a position x and an operator \mathbb{K} :

$$\mathbb{M}(x, \mathbb{K}) \equiv \begin{pmatrix} e^{i\mathbb{K}x} & e^{-i\mathbb{K}x} \\ \mathbb{K} e^{i\mathbb{K}x} & -\mathbb{K} e^{-i\mathbb{K}x} \end{pmatrix}. \quad (\text{A5})$$

Its inverse reads:

$$\mathbb{M}^{-1}(x, \mathbb{K}) = \frac{1}{2} \begin{pmatrix} e^{-i\mathbb{K}x} & \mathbb{K}^{-1} e^{-i\mathbb{K}x} \\ e^{i\mathbb{K}x} & -\mathbb{K}^{-1} e^{i\mathbb{K}x} \end{pmatrix} = \frac{1}{2} \mathbb{M}^\dagger(-x, \mathbb{K}^{-1}). \quad (\text{A6})$$

With these matrices the boundary conditions can be written as

$$\mathbb{M}(-L/2, \mathbb{K}_0) \begin{pmatrix} |a\rangle \\ |b\rangle \end{pmatrix} = \mathbb{M}(-L/2, \mathbb{K}) \begin{pmatrix} |a'\rangle \\ |b'\rangle \end{pmatrix} \quad (\text{A7})$$

$$\mathbb{M}(L/2, \mathbb{K}_0) \begin{pmatrix} |a''\rangle \\ |b''\rangle \end{pmatrix} = \mathbb{M}(L/2, \mathbb{K}) \begin{pmatrix} |a'\rangle \\ |b'\rangle \end{pmatrix}. \quad (\text{A8})$$

The transfer matrix \mathcal{M} is defined in equation (34) as the one that connects the amplitudes of the plane waves at the right and at the left sides of the scatterer (see figure 2). From the boundary conditions (A7) and (A8) one immediately gets

$$\mathcal{M} = \mathbb{M}^{-1}(L/2, \mathbb{K}_0) \mathbb{M}(L/2, \mathbb{K}) \mathbb{M}^{-1}(-L/2, \mathbb{K}) \mathbb{M}(-L/2, \mathbb{K}_0) \quad (\text{A9})$$

which is equation (35) in the main text.

Appendix B. Symmetries

B1. Conservation of probability current

If we write the scattering states in the following form

$$\langle x|\psi\rangle = \sum_J \psi_J(x)|s_J\rangle \quad (\text{B1})$$

and introduce this expression in the Schrödinger equation (29), we get

$$-\frac{1}{2m} \frac{\partial^2 \psi_J(x)}{\partial x^2} + (e_J - E)\psi_J(x) + \chi_L(x) \sum_K \psi_K(x) \langle s_J|H_{US}|s_K\rangle = 0. \quad (\text{B2})$$

The following generalization of the Wronskian

$$W(x) \equiv \sum_J \left[\frac{\partial \psi_J(x)}{\partial x} \psi_J^*(x) - \psi_J(x) \frac{\partial \psi_J^*(x)}{\partial x} \right] \quad (\text{B3})$$

can be interpreted as a total current of particles and is independent of x . To prove it, we use the Schrödinger equation to compute the derivative

$$\begin{aligned} \frac{dW(x)}{dx} &= \sum_J \left[\frac{\partial^2 \psi_J(x)}{\partial x^2} \psi_J^*(x) - \psi_J(x) \frac{\partial^2 \psi_J^*(x)}{\partial x^2} \right] \\ &= 2m \chi_L(x) \sum_{J,K} \left[\psi_K(x) \psi_J^*(x) \langle s_J|H_{US}|s_K\rangle - \psi_J(x) \psi_K^*(x) \langle s_J|H_{US}|s_K\rangle^* \right] = 0. \end{aligned} \quad (\text{B4})$$

To obtain the last equality, we have taken into account that H_{US} is self-adjoint and, consequently, the two terms in the sum are equal under a permutation of the indexes.

For a given total energy E , the solution (30) at $x \rightarrow -\infty$ corresponds to $\psi_J(x) = \alpha_J e^{ik_J x} + \beta_J e^{-ik_J x}$ if k_J is real ($e_J \leq E$) and $\psi_J(x) \simeq 0$ if k_J is imaginary ($e_J \geq E$). Then, the Wronskian reads

$$W(x) \simeq \sum_{J: e_J \leq E} 2ik_J [|\alpha_J|^2 - |\beta_J|^2]. \quad (\text{B5})$$

Similarly, for $x \rightarrow \infty$:

$$W(x) \simeq \sum_{J: e_J \leq E} 2ik_J [|\alpha_J''|^2 - |\beta_J''|^2]. \quad (\text{B6})$$

Therefore

$$\sum_{J: e_J \leq E} k_J [|\alpha_J|^2 - |\beta_J|^2] = \sum_{J: e_J \leq E} k_J [|\alpha_J''|^2 - |\beta_J''|^2]. \quad (\text{B7})$$

Notice that the sums in the previous expressions run only over the states $|s_J\rangle$ with k_J real, i.e. the incoming and outgoing plane waves.

The conservation of the total probability current (B7) imposes some constraints on the matrices \mathcal{M} and \mathcal{S} . Let \mathbb{P}_{open} be the projector onto $\mathcal{H}_{\text{open}}$, i.e. onto the eigenstates $|s_J\rangle$ with k_J real:

$$\mathbb{P}_{\text{open}} = \sum_{J: e_J \leq E} |s_J\rangle \langle s_J| \quad (\text{B8})$$

and let us define the operator acting on $[\mathcal{H}_{U,\text{int}} \otimes \mathcal{H}_S] \oplus [\mathcal{H}_{U,\text{int}} \otimes \mathcal{H}_S]$

$$\mathcal{P} = \begin{pmatrix} \mathbb{P}_{\text{open}} & 0 \\ 0 & \mathbb{P}_{\text{open}} \end{pmatrix}, \quad (\text{B9})$$

which verifies $\mathcal{P}^2 = \mathcal{P}$. Condition (B7) can be written as

$$(\langle a| \langle b|) \begin{pmatrix} \mathbb{K}_0 \mathbb{P}_{\text{open}} & 0 \\ 0 & -\mathbb{K}_0 \mathbb{P}_{\text{open}} \end{pmatrix} \begin{pmatrix} |a\rangle \\ |b\rangle \end{pmatrix} = (\langle a''| \langle b''|) \begin{pmatrix} \mathbb{K}_0 \mathbb{P}_{\text{open}} & 0 \\ 0 & -\mathbb{K}_0 \mathbb{P}_{\text{open}} \end{pmatrix} \begin{pmatrix} |a''\rangle \\ |b''\rangle \end{pmatrix}. \quad (\text{B10})$$

Applying the relationship (34) between the amplitudes of the waves at the right and left sides of the scatterer via the transfer matrix, we obtain

$$\begin{pmatrix} \mathbb{K}_0 & 0 \\ 0 & -\mathbb{K}_0 \end{pmatrix} \mathcal{P} = \mathcal{M}^\dagger \begin{pmatrix} \mathbb{K}_0 & 0 \\ 0 & -\mathbb{K}_0 \end{pmatrix} \mathcal{P} \mathcal{M} \quad (\text{B11})$$

and, multiplying by \mathcal{P} from right, we get

$$\mathcal{M}^\dagger \begin{pmatrix} \mathbb{K}_0 & 0 \\ 0 & -\mathbb{K}_0 \end{pmatrix} \mathcal{P} \mathcal{M} = \mathcal{M}^\dagger \begin{pmatrix} \mathbb{K}_0 & 0 \\ 0 & -\mathbb{K}_0 \end{pmatrix} \mathcal{P} \mathcal{M} \mathcal{P}. \quad (\text{B12})$$

Since \mathcal{M}^\dagger and \mathbb{K}_0 are both invertible in their respective Hilbert spaces (we assume that $k_j \neq 0$ for all j), we conclude that $\mathcal{P} \mathcal{M} \mathcal{P} = \mathcal{P} \mathcal{M}$ or $\mathcal{P} \mathcal{M} (\mathbb{I} - \mathcal{P}) = 0$. This relationship indicates that the amplitudes of the real exponentials (k_j imaginary) do not affect the amplitudes of the plane waves (k_j real) and that we can restrict ourselves to $\mathcal{H}_{\text{open}}$. Notice however that \mathcal{P} and \mathcal{M} do not necessarily commute, i.e. $\mathcal{H}_{\text{open}}$ is not in general invariant under the transfer matrix \mathcal{M} . However, the action of \mathcal{M} on vectors in $\mathcal{H}_{\text{open}}$ is entirely determined by its restriction to this subspace $\mathcal{P} \mathcal{M} \mathcal{P}$. In particular any power n of \mathcal{M} verifies $\mathcal{P} \mathcal{M}^n \mathcal{P} = (\mathcal{P} \mathcal{M} \mathcal{P})^n$ and the inverse of \mathcal{M} in $\mathcal{H}_{\text{open}}$ is $\mathcal{P} \mathcal{M}^{-1} \mathcal{P}$, that is $[\mathcal{P} \mathcal{M} \mathcal{P}][\mathcal{P} \mathcal{M}^{-1} \mathcal{P}] = [\mathcal{P} \mathcal{M}^{-1} \mathcal{P}][\mathcal{P} \mathcal{M} \mathcal{P}] = \mathcal{P}$. The same arguments apply to the matrix \mathcal{S} , which obeys $\mathcal{P} \mathcal{S} (\mathbb{I} - \mathcal{P}) = 0$. Hence, from now on, we can neglect the eigenstates $|s_j\rangle$ with imaginary k_j and explore the properties of the matrices \mathcal{M} and \mathcal{S} restricted to $\mathcal{H}_{\text{open}}$. Nevertheless, we will keep the same notation, for simplicity. Notice also that k'_j , the wave vectors within the scattering region $[-L/2, L/2]$, can be imaginary, indicating that the corresponding channel is associated with tunneling.

A second important consequence of the conservation of probability current is the unitarity of the scattering matrix. Condition (B7) can also be written as

$$(\langle a | \langle b'' |) \mathbb{K}_0 \begin{pmatrix} |a\rangle \\ |b''\rangle \end{pmatrix} = (\langle b | \langle a'' |) \mathbb{K}_0 \begin{pmatrix} |b\rangle \\ |a''\rangle \end{pmatrix} = (\langle a | \langle b'' |) \mathcal{S}^\dagger \mathbb{K}_0 \mathcal{S} \begin{pmatrix} |a\rangle \\ |b''\rangle \end{pmatrix} \quad (\text{B13})$$

where all vectors and operators are restricted to $\mathcal{H}_{\text{open}}$. Hence, $\mathbb{K}_0 = \mathcal{S}^\dagger \mathbb{K}_0 \mathcal{S}$ in this subspace and we finally obtain

$$\tilde{\mathcal{S}}^\dagger \tilde{\mathcal{S}} = \mathbb{K}_0^{-1/2} \mathcal{S}^\dagger \mathbb{K}_0^{1/2} \mathbb{K}_0^{1/2} \mathcal{S} \mathbb{K}_0^{-1/2} = \mathbb{I} \quad (\text{B14})$$

that is, the scattering matrix $\tilde{\mathcal{S}}$ is unitary.

B2. Spatial symmetry

The collision problem that we consider in this paper is invariant under spatial inversion $(x, p) \rightarrow (-x, -p)$, which is equivalent to the following transformation of vectors (see figure 2):

$$|a\rangle \leftrightarrow |b''\rangle \quad |b\rangle \leftrightarrow |a''\rangle. \quad (\text{B15})$$

This transformation converts equation (37) into

$$\begin{pmatrix} |a''\rangle \\ |b\rangle \end{pmatrix} = \mathcal{S} \begin{pmatrix} |b''\rangle \\ |a\rangle \end{pmatrix} \quad (\text{B16})$$

and comparing this expression with equation (37), we get

$$\begin{pmatrix} 0 & \mathbb{I} \\ \mathbb{I} & 0 \end{pmatrix} \mathcal{S} \begin{pmatrix} 0 & \mathbb{I} \\ \mathbb{I} & 0 \end{pmatrix} = \mathcal{S} \quad (\text{B17})$$

which yields $\mathcal{S}_{11} = \mathcal{S}_{22}$ and $\mathcal{S}_{12} = \mathcal{S}_{21}$. The same symmetry applies to the scattering matrix $\tilde{\mathcal{S}}$. This symmetry allows us to write the scattering matrix as in equation (10):

$$\tilde{\mathcal{S}} = \begin{pmatrix} \mathbf{r} & \mathbf{t} \\ \mathbf{t} & \mathbf{r} \end{pmatrix} \quad (\text{B18})$$

where \mathbf{r} and \mathbf{t} are matrices whose elements are the reflection and transmission amplitudes, respectively. The unitarity of $\tilde{\mathcal{S}}$ derived in equation (B14), can be written now as

$$\mathbf{r} \mathbf{r}^\dagger + \mathbf{t} \mathbf{t}^\dagger = \mathbb{I} \mathbf{r} \mathbf{t}^\dagger + \mathbf{t} \mathbf{r}^\dagger = 0 \quad (\text{B19})$$

which is equation (B14) in the main text.

B3. Time-reversal symmetry

The symmetry under time reversal implies that there is an anti-unitary operator T_{int} in the Hilbert space of internal states that commutes with H_0 and H_{US} . As discussed in the main text, the total time-reversal operator is $\mathsf{T} = \mathsf{T}_{U,p} \otimes \mathsf{T}_{\text{int}}$ where $\mathsf{T}_{U,p}$ is the conjugation of the wave function in the position representation. Hence, if $|\psi\rangle$ is given by (B1), then

$$\mathsf{T}|\psi\rangle = \sum_J \psi_J^*(x) \mathsf{T}_{\text{int}}|s_J\rangle. \quad (\text{B20})$$

For simplicity, we assume that the eigenstates of H_0 are invariant under time reversal, i.e. $\mathsf{T}_{\text{int}}|s_J\rangle = |s_J\rangle$. In this case, $[H_{US}, \mathsf{T}_{\text{int}}] = 0$ implies that $\langle s_J | H_{US} | s_K \rangle$ is real, that is, the matrix of the interaction Hamiltonian H_{US} in the eigenbasis of H_0 is real and symmetric. To prove this property, take into account that an anti-unitary operator verifies $(\mathsf{T}|a\rangle, \mathsf{T}|b\rangle) = (|a\rangle, |b\rangle)^*$, where (\cdot, \cdot) is the scalar product in the Hilbert space. Hence, we can take the complex conjugate of the Schrödinger equation (B2) and obtain the following transformation under time reversal for the vectors restricted to $\mathcal{H}_{\text{open}}$:

$$|a\rangle \leftrightarrow |b^*\rangle \quad |a''\rangle \leftrightarrow |b''^*\rangle \quad (\text{B21})$$

where $|b^*\rangle = \mathsf{T}|b\rangle = \sum_J \beta_J^* |s_J\rangle$. This symmetry implies

$$\begin{pmatrix} |a^*\rangle \\ |b''^*\rangle \end{pmatrix} = \mathcal{S} \begin{pmatrix} |b^*\rangle \\ |a''^*\rangle \end{pmatrix}. \quad (\text{B22})$$

Using (37), we obtain $\mathcal{S}^* \mathcal{S} = \mathbb{K}_0^{-1/2} \tilde{\mathcal{S}}^* \tilde{\mathcal{S}} \mathbb{K}_0^{1/2} = \mathbb{I}$, implying $\tilde{\mathcal{S}}^* \tilde{\mathcal{S}} = \mathbb{I}$, and

$$\begin{aligned} \mathbf{r}^* + \mathbf{t}^* &= \mathbb{I} \\ \mathbf{r}^* + \mathbf{t}^* &= 0. \end{aligned} \quad (\text{B23})$$

Combining this symmetry with the unitarity of the scattering matrix, equation (B19), we conclude $\mathbf{t}^\dagger = \mathbf{t}^*$ and $\mathbf{r}^\dagger = \mathbf{r}^*$, i.e. the matrices \mathbf{t} and \mathbf{r} are symmetric.

Appendix C. The high-energy limit

The matrix \mathcal{M} can be calculated exactly from equation (35). Here we introduce an approximation that preserves the symmetries and the unitarity of the scattering matrix and therefore provides a simple implementation of a thermal reservoir. The approximation is valid for incident particles with a large kinetic energy. In this case, we can approximate $\mathbb{K}^{-1} \mathbb{K}_0 \simeq \mathbb{I}$. Using this approximation and the expression for \mathbb{M} , (A5), and its inverse, equation (A6), we obtain

$$\begin{aligned} \mathbb{M}^{-1}(L/2, \mathbb{K}_0) \mathbb{M}(L/2, \mathbb{K}) &= \frac{1}{2} \begin{pmatrix} e^{-i\mathbb{K}_0 L/2} & \mathbb{K}_0^{-1} e^{-i\mathbb{K}_0 L/2} \\ e^{i\mathbb{K}_0 L/2} & -\mathbb{K}_0^{-1} e^{i\mathbb{K}_0 L/2} \end{pmatrix} \begin{pmatrix} e^{i\mathbb{K} L/2} & e^{-i\mathbb{K} L/2} \\ \mathbb{K} e^{i\mathbb{K} L/2} & -\mathbb{K} e^{-i\mathbb{K} L/2} \end{pmatrix} \\ &\simeq \begin{pmatrix} e^{-i\mathbb{K}_0 L/2} e^{i\mathbb{K} L/2} & 0 \\ 0 & e^{i\mathbb{K}_0 L/2} e^{-i\mathbb{K} L/2} \end{pmatrix} \end{aligned} \quad (\text{C1})$$

and

$$\begin{aligned} \mathbb{M}^{-1}(-L/2, \mathbb{K}) \mathbb{M}(-L/2, \mathbb{K}_0) &= \frac{1}{2} \begin{pmatrix} e^{i\mathbb{K} L/2} & \mathbb{K}^{-1} e^{i\mathbb{K} L/2} \\ e^{-i\mathbb{K} L/2} & -\mathbb{K}^{-1} e^{-i\mathbb{K} L/2} \end{pmatrix} \begin{pmatrix} e^{-i\mathbb{K}_0 L/2} & e^{i\mathbb{K}_0 L/2} \\ \mathbb{K}_0 e^{-i\mathbb{K}_0 L/2} & -\mathbb{K}_0 e^{i\mathbb{K}_0 L/2} \end{pmatrix} \\ &\simeq \begin{pmatrix} e^{i\mathbb{K} L/2} e^{-i\mathbb{K}_0 L/2} & 0 \\ 0 & e^{-i\mathbb{K} L/2} e^{i\mathbb{K}_0 L/2} \end{pmatrix}, \end{aligned} \quad (\text{C2})$$

yielding

$$\mathcal{M} \simeq \begin{pmatrix} e^{-i\mathbb{K}_0 L/2} e^{i\mathbb{K} L} e^{-i\mathbb{K}_0 L/2} & 0 \\ 0 & e^{i\mathbb{K}_0 L/2} e^{-i\mathbb{K} L} e^{i\mathbb{K}_0 L/2} \end{pmatrix} \quad (\text{C3})$$

which is equation (38) in the main text.

Appendix D. Properties of the two-qubit example

Here we explicitly derive some properties of the example studied in section 5. The total internal Hamiltonian H in the eigenbasis of the free Hamiltonian (56), ordered as $\{|00\rangle_{US}, |01\rangle_{US}, |10\rangle_{US}, |11\rangle_{US}\}$, reads

$$H = H_0 + H_{US} = \begin{pmatrix} \Omega & 0 & 0 & \xi \\ 0 & \Delta\omega & \Xi & 0 \\ 0 & \Xi & -\Delta\omega & 0 \\ \xi & 0 & 0 & -\Omega \end{pmatrix} \quad (D1)$$

where $\Omega = \omega_S + \omega_U$, $\Delta\omega = \omega_U - \omega_S$, $\Xi = J_x + J_y$, and $\xi = J_x - J_y$. The block structure of this matrix allows only for transitions $|11\rangle_{US} \leftrightarrow |00\rangle_{US}$ and $|10\rangle_{US} \leftrightarrow |01\rangle_{US}$. The eigenvalues of H are $\pm\sqrt{\Omega^2 + \xi^2}$ and $\pm\sqrt{\Delta\omega^2 + \Xi^2}$.

If $J_x = J_y$, then $\xi = 0$ and the only permitted transitions are the swaps $|10\rangle_{US} \leftrightarrow |01\rangle_{US}$ and the probability that the system jumps from 0 to 1 in the RIT model with $\tau_{\text{packet}}(p_0) \equiv Lm/p_0$ reads:

$$p(j_S = 0 \rightarrow j'_S = 1) = \frac{e^{-\beta\omega_U}}{Z_U} \int_{\sqrt{2me_{\max}}}^{\infty} dp_0 \mu(p_0) \langle 01 | e^{-i\tau_{\text{packet}}(p_0)H} | 10 \rangle \quad (D2)$$

whereas

$$p(j_S = 1 \rightarrow j'_S = 0) = \frac{1}{Z_U} \int_{\sqrt{2me_{\max}}}^{\infty} dp_0 \mu(p_0) \langle 10 | e^{-i\tau_{\text{packet}}(p_0)H} | 01 \rangle. \quad (D3)$$

Then, the ratio verifies

$$\frac{p(j_S = 0 \rightarrow j'_S = 1)}{p(j_S = 1 \rightarrow j'_S = 0)} = e^{-\beta\omega_U} \quad (D4)$$

and the system thermalizes in the resonant case, $\omega_U = \omega_S$, where heat is identically zero.

On the other hand, if $J_x = -J_y$, then $\Xi = 0$ and the only permitted transitions are $|00\rangle_{US} \leftrightarrow |11\rangle_{US}$. Hence

$$p(j_S = 1 \rightarrow j'_S = 0) = \frac{e^{-\beta\omega_U}}{Z_U} \int_{\sqrt{2me_{\max}}}^{\infty} dp_0 \mu(p_0) \langle 00 | e^{-i\tau_{\text{packet}}(p_0)H} | 11 \rangle \quad (D5)$$

whereas

$$p(j_S = 0 \rightarrow j'_S = 1) = \frac{1}{Z_U} \int_{\sqrt{2me_{\max}}}^{\infty} dp_0 \mu(p_0) \langle 11 | e^{-i\tau_{\text{packet}}(p_0)H} | 00 \rangle. \quad (D6)$$

Now the ratio verifies

$$\frac{p(j_S = 0 \rightarrow j'_S = 1)}{p(j_S = 1 \rightarrow j'_S = 0)} = e^{\beta\omega_U} \quad (D7)$$

which indicates that the steady state exhibit a population inversion with negative absolute temperature, as shown in figure 4.

ORCID iDs

Jorge Tabanera  <https://orcid.org/0000-0001-8706-6886>

Felipe Barra  <https://orcid.org/0000-0001-9346-2826>

Juan M R Parrondo  <https://orcid.org/0000-0001-8525-3709>

References

- [1] Spohn H and Lebowitz J L 1978 Irreversible thermodynamics for quantum systems weakly coupled to thermal reservoirs *Advances in Chemical Physics* (New York: Wiley) pp 109–42
- [2] Breuer H-P and Petruccione F 2007 *The Theory of Open Quantum Systems* (Oxford: Oxford University Press)
- [3] Rivas A and Susana H 2012 *Open Quantum Systems: An Introduction* (Heidelberg: Springer)
- [4] Dann R, Levy A and Kosloff R 2018 *Phys. Rev. A* **98** 052129
- [5] Paternostro M, De Chiara G, Ferraro A, Campisi M, Goold J, Semiao F L, Plastina F and Vedral V 2019 *J. Stat. Mech.* **104014**
- [6] Hofer P P, Perarnau-Llobet M, Miranda L D M, Haack G, Silva R, Brask J B and Brunner N 2017 *New J. Phys.* **19** 123037
- [7] Strasberg P 2019 *Phys. Rev. Lett.* **123** 180604
- [8] Rivas Á 2020 *Phys. Rev. Lett.* **124** 160601
- [9] Breuer H-P, Laine E-M, Piilo J and Vacchini B 2016 *Rev. Mod. Phys.* **88** 021002
- [10] Barra F 2015 *Sci. Rep.* **5** 1–10
- [11] Strasberg P, Schaller G, Brandes T and Esposito M 2017 *Phys. Rev. X* **7** 021003
- [12] Seah S, Nimmrichter S and Scarani V 2019 *Phys. Rev. E* **99** 042103
- [13] Guarnieri G, Morrone D, Cakmak B, Plastina F and Campbell S 2020 *Phys. Lett. A* **384** 126576